



室蘭工業大学

学術資源アーカイブ

Muroran Institute of Technology Academic Resources Archive



Shear Resisting Behavior of Short Reinforced Concrete Columns under Biaxial Bending-Shear and Varying Axial Load

メタデータ	言語: eng 出版者: Japan Concrete Institute 公開日: 2012-07-18 キーワード (Ja): キーワード (En): 作成者: 溝口, 光男, 荒川, 卓, 荒井, 康幸, 吉田, 稔 メールアドレス: 所属:
URL	http://hdl.handle.net/10258/1289

SHEAR RESISTING BEHAVIOR OF SHORT REINFORCED CONCRETE COLUMNS
UNDER BIAXIAL BENDING-SHEAR AND VARYING AXIAL LOAD

Mitsuo MIZOGUCHI*¹, Takashi ARAKAWA*¹, Yasuyuki ARAI*¹ and Minoru YOSHIDA*²

ABSTRACT

The effect of biaxial bending-shear force reversals and varying axial load on the shear resisting behavior of short reinforced concrete columns was experimentally investigated. The short columns with square section were cyclically deflected along their principal axes and their diagonals to produce biaxial bending-shear under uniaxial loadings. The results from 10 tests were considered. It was concluded that the shear strength of short columns under varying axial load could be estimated using existing empirical formulae and, in case of high axial stress, the shear strength of column loaded diagonally was 5~6 % lower than that of the column loaded along the principal axis.

1. INTRODUCTION

The experimental research on shear behavior of short reinforced concrete (RC) columns under constant axial load and unidirectional load reversals has been conducted by many investigators. Real exterior and corner columns in the first storey of highrise RC buildings are subjected to varying axial load due to the earthquake overturning moment, in addition to biaxial lateral loadings. However, there are very few data on the shear resisting behavior for these short RC columns.

In this paper, 10 specimens were tested to examine the influences of varying axial load histories and biaxial bending-shear forces on the shear behavior of short square columns. The main variables were three kinds of lateral loading direction (unidirectional loading, diagonal 45° and 22.5° loading from the principal axis) and four kinds of fluctuating axial load.

2. EXPERIMENTAL PROGRAM

2.1 TEST SPECIMENS

Ten fifth-scale column specimens as shown in Fig.1 were tested. All specimens had a 18 cm square section with eight D13 longitudinal bars (gross reinforcement ratio P_g of 3.14 %) and 4-mm transverse reinforcement. The cross section of the test column was so determined that a high compressive stress

*¹ Department of Civil Engineering and Architecture, Muroran Inst. of Tech.

*² Ohbayashi Corporation

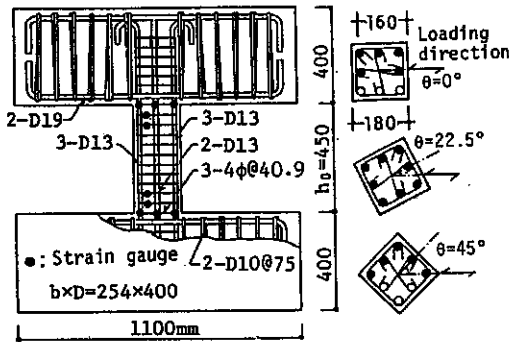


Fig.1 Details of specimen

($\sigma_c = N/bD = 150 \text{ kgf/cm}^2$) could be produced by hydraulic actuator with capacity of 50 tonf. In order to ensure that shear behavior was controllable, a short column (clear height-thickness ratio, $h_0/D=2.5$) with low percentage of transverse reinforcement ($P_w=0.50\%$) was selected. The design compressive strength of concrete (F_c) was 300 kgf/cm^2 .

The specimens were named according to the loading condition as listed in Table 1. The first numerals indicate the angle of loading to the principal axis; '0' is uniaxial lateral loading ($\theta=0^\circ$ or 90°), '2' and '4' are biaxial loading with 22.5° and 45° from the principal axis. The second marks 'V' and 'VA' present the varying axial load as shown in Figs.2 (a) and (b). The third numerals '04' and '15' present the fluctuating range of axial stress ratio ($\eta = N/bD\sigma_B$, σ_B is the compressive strength of concrete obtained from the test); '0' is no axial load, '1' is axial tension of $\eta = -0.1$, '4' and '5' represent $\eta = 0.4$ and $\eta = 0.5$, respectively.

As for the V04 and V15-type columns shown in Fig.2 (a), the axial load was varied proportional to the column shear forces (Q). The value of $\eta = 0.2$ was assumed as the basic axial stress ratio. The maximum and minimum axial loads were determined to develop as the column shear forces reach about 75 % of the ultimate shear strength calculated by the existing formula ($Q = -5$ & 10 tonf). On the other hand, the VA04 and VA15-type columns shown in Fig.2 (b) were prepared to compare with those subjected to constant axial load and unidirectional lateral load reversals(1).

Table 1 Test specimens

Varying of η	(-) (-)	(+) (+)	(-) (-)	(+) (+)	(-) (-)	(+) (+)
	0-0.2-0.4	0.1-0.2-0.5	0 - 0.4	0.1 - 0.5	0.1 - 0.5	0.1 - 0.5
$\theta = 0^\circ$	0V04	0V15	0VA04	0VA15	—	—
$= 22.5^\circ$	2V04	—	2VA04	—	—	—
$= 45^\circ$	4V04	4V15	4VA04	4VA15	—	—

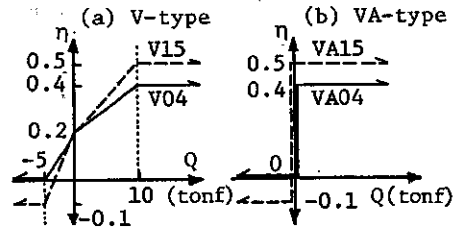


Fig.2 Varying axial load

2.2 MECHANICAL PROPERTIES AND FABRICATION OF SPECIMENS

Mechanical properties of the specimens are summarized in Table 2. All specimens were horizontally cast in steel forms. Three days after casting concrete the specimens and the control cylinders (diameter=10 cm, height=20 cm) were demolded, and then kept continuously wet and covered with polyethylene sheets until 70 % of concrete design strength was attained. The specimens were tested at the age of 29~39 days.

Table 2 Mechanical properties

Size	Reinforcement			Concrete
	As (cm ²)	σ_y (kgf/cm ²)	Es (x10 ⁶ kgf/cm ²)	
4φ	0.123	2790	2.11	w/c = 60% by weight, 1 : 2.65 : 3.46 s1.=18cm, Sand ≤ 2.5, Gravel ≤ 10mm $\sigma_B=291$, $\sigma_t=31.2 \text{ kgf/cm}^2$, $E_c=2.62 \times 10^5 \text{ kgf/cm}^2$
D10	0.713	3600	—	
D13	1.267	3490	1.81	
D19	2.865	3630	—	

2.3 LOADING HISTORY AND LOADING APPARATUS

The loads were controlled in a deflection mode for the lateral history and in a load mode for the axial force. In each specimen the lateral load reversals were applied after the axial force was introduced. As shown in Fig.3, the deflection increment in each cycle (Δ) was 0.9 mm (rotation angle R was defined as the lateral displacement δ divided by the column height h_0 , $R=2 \times 10^{-3}=1/500$ rad.) and the displacement was increased progressively from the beginning to the end of a total of 12 cycles ($\delta=10.8$ mm, $R=24 \times 10^{-3}=1/40$ rad.).

Figure 4 shows a elevation view of the loading apparatus. Axial and lateral loads were applied to an L-shaped loading frames by hydraulic actuators ② and ③, respectively. Actuator ① was used for keeping the upper and lower loading beams horizontal. The influence of the angular deviation of vertical braces on the lateral shear force was considered. Three horizontal braces were used for restraining the specimen from rotating in the direction normal to the loading plane during loading as shown by solid square marks in Fig.4.

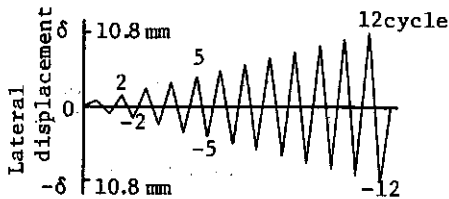


Fig.3 Cyclic loading history

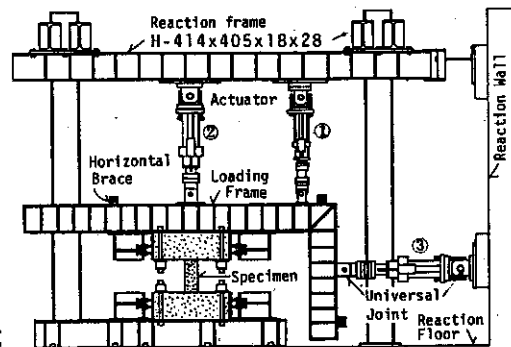


Fig.4 Loading apparatus

2.4 INSTRUMENTATION AND TEST PROCEDURE

The applied lateral and axial loads were measured by load cells which were incorporated in the loading and restraining actuators ① to ③. In order to obtain the lateral displacement in the loading direction of column, two pairs of four linear variable differential transducers were positioned on both sides at the mid-depth of the upper and lower beams. The same kind of six linear transducers were used for measuring axial displacements between the upper and lower beams. Strains in longitudinal and transverse reinforcement were measured by wire resistance strain gages (gage length=2 mm), as shown in Fig.1 by solid circle marks. Load-deflection curves and strains were recorded by personal computer and disk memory at each load stage, and also crack patterns were traced and photographed.

3. TEST RESULTS AND DISCUSSION

3.1 FRACTURE PROCESSES

The applied axial load for a specimen is basically different between the positive and negative loading. Therefore, the crack pattern, failure mode and load-deflection relationship in each specimen are not symmetric as shown in Figs.5 and 6.

In the positive loading, flexural cracks occurred in the 1st cycle at the both ends of the column. And then the diagonal steeper cracks appeared along the longitudinal middle bar arranged at the mid-depth of column cross section in the 2nd to 3rd (3rd cycle: for specimens of 2VA04 and 4VA04) cycles.

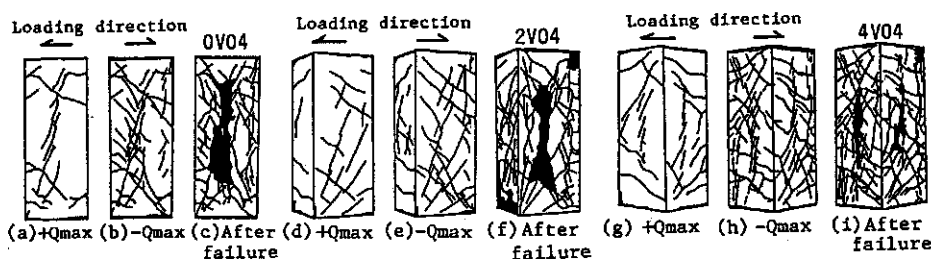


Fig.5 Cracking pattern and after failure

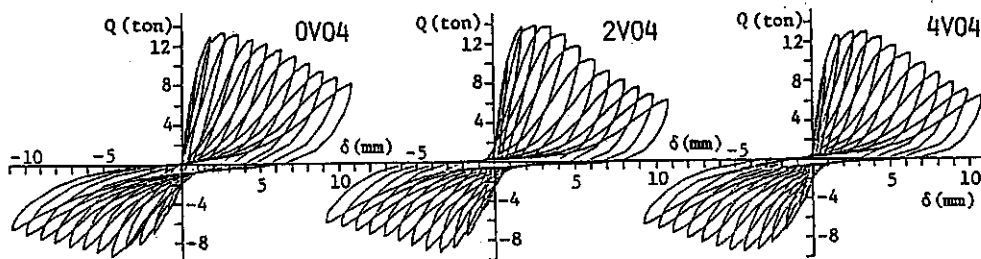


Fig.6 Load-displacement curves

These shear cracks extended and a little widened in the 3rd to 4th cycles. At the same cycle, the maximum lateral loads were attained for all specimens as shown in Figs.5 (a), (d) and (g).

With further increase in loading cycles, existing cracks widened and bond cracks along the longitudinal bars extended with spalling of cover concrete, and the load carrying capacity of column reduced gradually as shown in Fig.6. The crack patterns for the columns subjected to unidirectional loading and varying axial load resemble each other. However, for diagonally loaded columns, these cracks were widely extended to all face of column.

On the other hand, in the negative loading, because the applied axial load of column varied from compression to zero or tension, the characteristics of cracking appearance and extension are different from those of the positive loading. All test columns underwent flexural cracking, flexurel-shear cracking and diagonal shear cracking at the surface of the column. In case of the OVA15 and 4VA15 columns subjected to axial tension, the horizontal tension cracks perpendicular to the longitudinal axis appeared at almost equal intervals. The diagonal shear cracks with more gentle slope than those in case of the positive loading were distributed widely along all height of the column. These shear cracks extended with increase in the displacement level or added cycles. The maximum lateral loads in all specimens were attained at the 4th to 6th negative cycles as shown in Fig.5 (b), (e) and (h).

The crack patterns for columns under unidirectional loading and varying axial load were similar to each other. However, for the diagonally loaded columns, the shear cracks formed at the maximum loads in the negative cycle were distributed more widely range than in the OV or OVA-type columns. With further increase in negative loading cycles, the load carrying capacity of column decreased gradually with spalling of cover concrete along the longitudinal middle bar as shown in Figs.5 (c), (f) and (i).

3.2 STRAINS OF LONGITUDINAL AND TRANSVERSE REINFORCEMENT

The measured maximum shear capacity for the column loaded uniaxially was always reached before the longitudinal reinforcement yielded. However, for the column loaded diagonally, the corner longitudinal reinforcements were yielded in compression before reaching maximum shear in the positive loading.

All transverse reinforcement placed at the position of $d/2$ from the top and bottom ends of column yielded at the maximum shear in the positive loading.

3.3 LOAD-DISPLACEMENT RELATIONSHIPS

(1) Load-displacement envelope curves

Envelope curves are presented so as to compare the test results without showing the entire measured cyclic load-displacement relationships. The envelope curves for all columns are shown in Figs.7 (a), (b) and (c). The measured lateral load (shear force Q) was normalized as $Q/bD(180+\sigma_B)$, where, bD is the cross sectional area of column and $(180+\sigma_B)$ is a parameter introduced to provide a reasonable relationship between concrete strength and shear strength with reference to the existing formula (see Eq.4).

As can be seen, for columns subjected to axial tension, the load carrying capacity after reaching maximum shear decreased slightly in the negative loadings, but there are almost no influences of varying axial load and diagonal loadings.

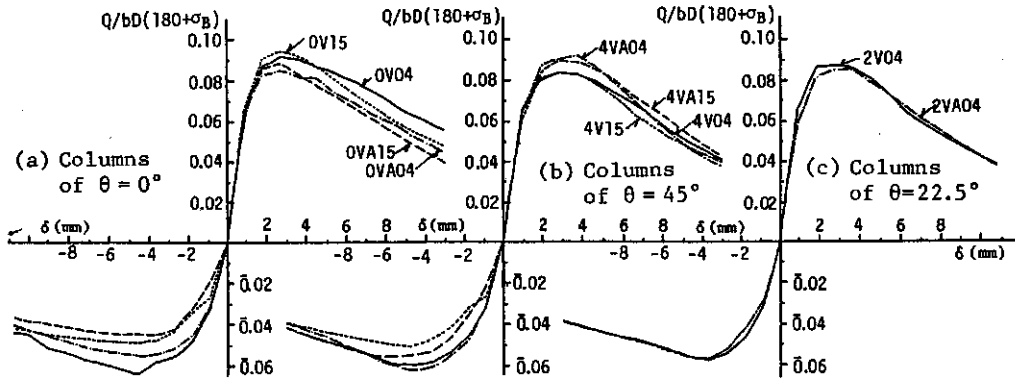


Fig.7 Load-displacement envelope curves

(2) Normalized hysteresis loops

As a typical example, Fig.8 shows the normalized hysteresis loops at the maximum shear and 12th cycles after failure. The configuration of hysteresis loops at the positive and negative cycles differed each other. However, these loops showed definite pinching toward the origin, "the inverted S-shape," which is characteristic of shear behavior of the columns. These behavior are observed for all columns. And significant differences due to the varying axial load and diagonal loading are not observed.

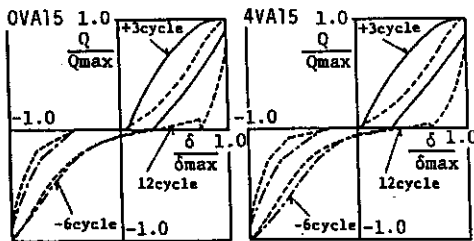


Fig.8 Normalized hysteresis loops

(3) Axial displacements

Figure 9 shows the comparison of axial displacement-lateral de-

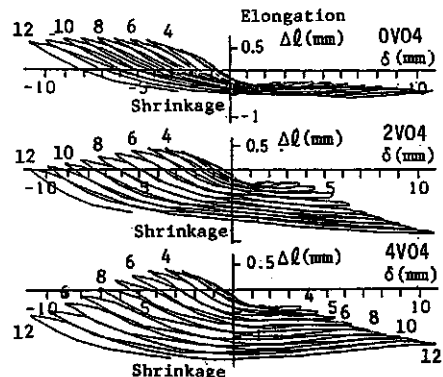


Fig.9 Axial displacement-lateral deflection relationship

flection relationship for 0V04, 2V04 and 4V04 columns with different loading direction. The axial displacement (Δl) of 0V04 column showed almost a constant value and was very stable even if increase of cyclic number and cyclic lateral deflection (δ). On the contrary, for the 2V and 4V-type columns loaded diagonally, the axial compressive deformations in both positive and negative cycles increased with increase of cyclic numbers and showed unstable behavior accompanied with the crushing of corner concrete at the both ends of column.

3.3 CRACKING STRENGTH

(1) Flexural cracking load

Figure 10 (a) shows the results of the influence of axial stress ratio η on the flexural cracking load. In this figure, the dotted line shows a value obtained from Eq.(1) assuming that $\sigma_B=300$ kgf/cm². Test results are good agreement with the computed value.

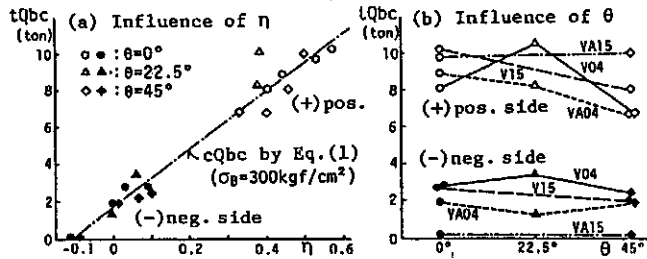
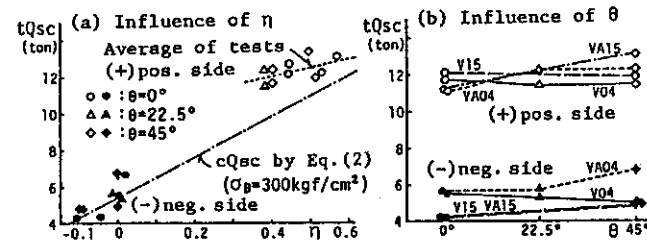


Figure 10 (b) shows the results of the influence of the loading direction angle θ . In the positive cycle, the test results are decreased slightly with increase of θ . However, there are almost no influence of the loading direction in the negative cycle. As listed in Table 3, the test results are in agreement with the computed value (cQbc) from Eq.(1), in which the effect of the loading angle θ was ignored.

Fig.10 Flexural cracking load

(2) Shear cracking load

As shown in Fig.11 (a), the test results in the negative loading approximated to the strength (cQsc) obtained from Eq.(2).



However, the test results in the positive loading were a little higher value than the value obtained from Eq.

Fig.11 Shear cracking load

(2). The ratios of the test results to the computed value by Eq.(2), in which the effect of the loading angle θ was ignored, are listed in Table 3. The average value of ratios was 1.21 (1.10~1.33, standard deviation is 0.068) at the positive loading and 1.03 (0.93~1.25, standard deviation is 0.092) at the negative loading. The effect of loading angle on the shear cracking strength is not recognized as shown in Fig.11(b).

3.4 ULTIMATE SHEAR STRENGTH

The measured maximum shear strength tQ_{su} exceeded about 25 % for the positive loading and about 10 % for the negative loading, respectively, the calculated flexural strength tQ_{fu} by Eq.(3). In this case, the calculation was made in assuming no effect of loading angle.

Figure 12 shows a relationship between axial stress ratio η and loading direction angle θ . As shown in Fig.12 (a), the experimental results are in best agreement with the calculated values by Eq.(4) which considers the influence of η . In case of the positive loading, the average value of ratios(x) of the measured to the calculated shear strength by Eq.(4) is equal to 1.00 and the standard deviation(σ) is equal to 0.036. In case of negative

Table 3 Test results

Column No.	σ_B (σ_t) (kgf/cm ²)	loading	At cracking load						At maximum load					
			η	tQbc (tf)	tQbc cQbc	η	tQsc (tf)	tQsc cQsc	η	tQsu (tf)	tQsu cQsu	tQsu cVmu	R(rad.) x10	
OV04	270 (29.9)	+	0.400	8.1	1.01	0.444	12.7	1.33	0.444	13.41	1.03	1.21	1.06	6.02
		-	0.093	2.8	0.89	0.017	5.7	1.07	0	9.33	1.04	0.91	0.93	10.02
OV15	263 (29.7)	+	0.570	10.3	0.99	0.570	13.1	1.25	0.570	13.66	1.06	1.26	1.11	6.02
		-	0.030	2.9	1.34	-0.046	4.3	0.93	-0.114	7.02	0.91	0.81	0.77	10.00
OVA04	274 (29.6)	+	0.438	8.9	1.03	0.439	12.1	1.26	0.438	13.07	1.00	1.17	1.02	5.87
		-	0	1.9	1.12	0	5.6	1.05	0	8.15	0.90	0.79	0.80	10.00
OVA15	280 (29.4)	+	0.536	9.7	0.99	0.535	12.2	1.13	0.536	13.32	1.01	1.17	1.02	5.27
		-	-0.107	0.2	-	-0.107	4.3	1.00	-0.107	6.71	0.85	0.77	0.70	12.00
2V04	312 (31.8)	+	0.385	10.4	1.49	0.385	11.6	1.15	0.385	13.89	1.00	1.12	0.98	6.02
		-	0.061	3.4	1.29	0	5.4	0.96	0	9.26	0.96	0.86	0.83	8.02
2VA04	317 (34.4)	+	0.379	8.3	1.18	0.379	12.4	1.26	0.379	13.73	0.98	1.10	0.96	7.80
		-	0	1.3	0.71	0	5.7	1.01	0	9.26	0.95	0.85	0.82	8.04
4V04	301 (34.2)	+	0.336	6.8	1.11	0.399	11.7	1.18	0.399	13.00	0.95	1.08	0.94	6.02
		-	0.106	2.4	0.76	0	5.0	0.91	0	9.39	0.99	0.88	0.86	10.02
4V15	291 (31.8)	+	0.457	8.1	1.08	0.515	12.0	1.10	0.515	12.74	0.95	1.09	0.95	5.89
		-	0.072	2.1	0.79	-0.088	4.8	1.06	-0.103	7.71	0.95	0.87	0.78	10.02
4VA04	299 (31.3)	+	0.401	6.8	0.98	0.402	12.4	1.25	0.401	14.21	1.04	1.19	1.04	8.02
		-	0	1.9	1.07	0	6.9	1.25	0	9.79	1.04	0.92	0.91	10.02
4VA15	302 (29.9)	+	0.497	10.0	1.21	0.496	13.3	1.20	0.497	14.03	1.02	1.16	1.01	6.02
		-	-0.099	0.1	-	-0.099	4.8	1.08	-0.099	8.75	1.06	0.98	0.86	5.41

Flexural cracking strength(2): $cMbc = 1.8\sqrt{\sigma_B}Ze + NZe/Ac$, $cQbc = 2cMbc/h_0$ (1)

Shear cracking strength(2): $oAQsc = \{0.085 kc (\sigma_B + 500) / (M/Qd + 1.7)\} b j$, $cQsc = (1 + \sigma_0/150) oAQsc$... (2)

Ultimate flexural strength(2): $cQfu = \{0.81 \alpha_t s \sigma_y D + 0.5ND(1 - \frac{N}{bD\sigma_B}) + 2\alpha_t s \sigma_y D(\frac{2d}{D} - \frac{N}{bD\sigma_B} - \frac{0.52\alpha_t s \sigma_y}{bD\sigma_B})\} \frac{2}{h_0}$ (3)

Ultimate shear strength(2): $cQsu = (0.9 + \sigma_0/250) oAQsu$, ($\sigma_0 \leq 150$ kgf/cm²)(4)

$oAQsu = \{ \frac{0.115ku kp(\sigma_B + 180)}{(M/Qd + 0.12)} + 2.7\sqrt{Fw\sigma_wy} \} b j$

AIJ Design Guideline(3): $AVu = Pw\sigma_wy b j_t \cot\phi + \tan\theta(1 - \beta) bD\sigma_B/2$ (5)

AIJ Commentary Eq. 6.9(3): $cVu = Pw\sigma_wy b j_t + \tan\theta(2Y/\tan\theta - \beta) bD\sigma_B/2$ (6)

Modified AIJ Equation(1): $cVmu = Pw\sigma_wy b j_t + (1 + \eta)\tan\theta(1 - \beta) bD\sigma_B/2$, ($\eta \leq 0.4$)(7)

loading, it is indicated that $\eta=0.97$ and $\sigma=0.065$.

On the other hand, the calculated shear strength AVu obtained from Eq.(5) which is proposed by the AIJ (3), shows conservative value for the column with high axial stress in the positive loading, but the value of AVu indicates oppositely a little overestimate for the column with axial tension or no axial load in the negative loading. For the allowable temporary column shear force QAS prescribed in the AIJ Standard(4), all experimental results in both positive and negative loading are plotted at more than calculated value $QAS=3.57$ tonf.

On the influence of the θ , no particular change is recognized at the positive loading as shown in Fig.12 (b), but the measured maximum shear strength at the negative loading had a tendency to show only slightly high value in proportion to θ .

Table 4 shows a comparison of the measured maximum shear strength for column loaded diagonally with that for column loaded unidirectionally along the principal axis. In this Table, Eqs.(4) and (7) are used to calculate the shear strength of column. The rates of reduction in the maximum shear strength on the basis of the column loaded along principal axis are indicated by the numerical value in a parenthesis.

As can be seen, in the positive loading, the rate of reduction in the maximum shear strength of column with diagonal loading was about 5~6 % as same

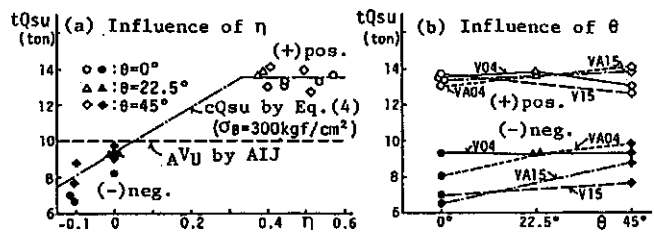


Fig.12 Ultimate shear strength

Table 4 Comparison of reduction rate in ultimate shear strength

Ratio	θ	$\theta = 0^\circ$	$\theta = 22.5^\circ$	$\theta = 45^\circ$
$\frac{tQ_{su}}{cQ_{su}}$	pos. (+)	1.00~1.06, m=1.03 (1.00)	0.98~1.00, m=0.99 (0.96)	0.95~1.04, m=0.99 (0.96)
	neg. (-)	0.85~1.04, m=0.93 [1.00]	0.95~0.96, m=0.96 [1.03]	0.95~1.06, m=1.01 [1.09]
$\frac{tQ_{su}}{cV_{mu}}$	pos. (+)	1.02~1.11, m=1.05 (1.00)	0.96~0.98, m=0.97 (0.92)	0.94~1.04, m=0.99 (0.94)
	neg. (-)	0.70~0.93, m=0.80 [1.00]	0.82~0.83, m=0.83 [1.03]	0.78~0.91, m=0.85 [1.07]
Average,	pos. (+)	m=1.04 (1.00)	m=0.98 (0.94)	m=0.99 (0.95)
	neg. (-)	m=0.87 [1.00]	m=0.90 [1.03]	m=0.93 [1.07]

as the previous report(1). On the other hand, in the negative loading, the ratios of experimental results to calculated values showed tendency of slightly increasing in proportion to the loading direction angle θ .

4. CONCLUSION

Based on the results of this study the following conclusions were made:

(1) The crack pattern, failure mode and load-displacement relationships in each columns were not symmetric, because the applied axial stress varied from compression to zero or tension. The diagonal cracks showed a tendency to become steeper with increase of axial stress.

(2) The ultimate shear strength of short columns could be estimated by Eq.(4), regardless of loading direction and axial load. Therefore, it was necessary to consider the factor of η in the design equation proposed by AIJ.

(3) In case of high axial stress at the positive loading, the shear strength of columns loaded diagonally was 5~6 % lower than that of column loaded along the principal axis. In case of low axial stress or tensile stress at the negative loading, the shear strength was conversely higher 3~7 %.

ACKNOWLEDGEMENT

This investigation was supported by the 1989's Grant-in-Aid for Scientific Research, Ministry of Education, Science and Culture of Japan. The experimental program was performed at the Muroran Institute of Technology. The authors wishes to express their gratitude to graduate student Mr.N. Ogawa and Mr.M. Matsuoka for their assistant in this investigation.

REFERENCES

- (1) Arakawa, T., et al., "Shear Resisting Behavior of Short Reinforced Concrete Columns under Biaxial Bending-Shear," Trans. of JCI, Vol. 11, 1989, pp. 317~324.
- (2) AIJ, "Data for Ultimate Strength Design of Reinforced Concrete Structures," 1987, pp. 36~37, 70 & 81 (in Japanese).
- (3) AIJ, "Design Guideline for Earthquake Resistant Reinforced Concrete Buildings Based on Ultimate Strength Concept," 1988, pp. 112~129 (in Japanese).
- (4) AIJ, "AIJ Standard for Structural Calculation of Reinforced Concrete Structures," 1985, 32~37.